Characterization of aerosol particle size distribution measurements by fitting lognormal functions during an aerosol acoustic agglomeration process

Manuel Aleixandre[1], Enrique Riera[1], Juan A. Gallego-Juárez[1], Rosario Delgado-Tardáguila[2] and Luis E. Herranz[2]

[1] Dpto. Sensores y Tecnologías Ultrasónicas (DSSU), ITEFI, CSIC, Madrid, Spain.
manuel.aleixandre@csic.es, enrique.riera@csic.es, j.gallego@csic.es
[2] Unidad de Seguridad Nuclear, División de Fisión Nuclear, CIEMAT, Madrid, Spain
rosario.delgado@ciemat.es, luisen.herranz@ciemat.es

Abstract
Aerosol particles inside a high-amplitude ultrasonic field can experience an agglomeration process that causes their size distribution to be changed. The overall effect of this process can be measured by the particle diameter growth, in terms for instance of the Aerodynamic Count Median Diameter (ACMD). However, the analysis of a poly-dispersed particle mixture requires a complex evaluation of the aerosol size distribution. In this work a method consisting on fitting the measured aerodynamic particle size distributions by lognormal functions is proposed. The aerosols used in the experiments were composed by SiO2 particles of different sizes: 0.3 µm, 1 µm, and 2.5 µm, with different concentrations and exposed to a intense ultrasonic standing wave field with an average sound pressure level of about 155 dB and a frequency of 21 kHz.

Keywords: Power Ultrasounds, Aerosol, Agglomeration, Curve fitting.

PACS no. 02.60.Ed, 43.35.+d

1   Introduction

The field of power ultrasound has a great potential for environmental and industrial applications [1]. One of these applications is the Acoustic Aerosol Agglomeration (AAA) [2]. The idea of the acoustic agglomeration was first experimentally investigated with high intensity ultrasound by Patterson and Cawood in 1931 [3] and its mechanisms have been extensively studied over many years. The first attempts of its use to clean up emissions from power plants and chemical industries were carried out during the second half of the last century .Throughout this period the technology has evolved and new devices based on ultrasonic plate-transducers with high efficiency and power capacity have been developed [4]. Such new devices and their higher efficiency allow the difficult process of aerosol cleaning to be feasible, mainly for the very small particles (below 2 µm), because the increase of the particle size due to the ultrasonic agglomeration facilitates the aerosol deposition, filtering, or retention [2]. This ultrasonic technology, based on the new generation devices, could facilitate the use of the AAA process at industrial level for removing aerosols produced in coal or diesel power plants [5], or even in nuclear plants in case of accidents [6]. This work, founded by the EU-PASSAM project

(Grant agreement No. 323217 – Euratom 7FP), studies the AAA process for its application to pre conditioning for clean up aerosols produced during severe nuclear accident [7].

The AAA is a process in which an acoustic field induces in the aerosol particles a relative motion that leads to collisions and agglomeration. The particle relative movements can be described by different mechanisms that are detailed in several works [8-11]. One important acoustic induced agglomeration mechanism is the orthokinetic effect. According to this simple mechanism particles with different sizes or densities follow the acoustic field with different entrainment, moving at different amplitude, vibration velocity and phase. The movement produces collisions and agglomeration that modify the overall aerosol particle number size distribution.

To measure the aerosol size distribution there are several experimental techniques. Most of these techniques have in common that they classify the particles according to their size (grouping them in bins) and then measure the amount of particles in each bin size. In the inertial impactors the particles are carried by a flow in a curvilinear trajectory and depending on their Stokes number they are collected in different stages according to their aerodynamic size. The particles in each stage can be counted by different methods such as by weight (weighting the collected particles) or by current (charging the particles at the inlet) [12]. Other methods are based on the electrical mobility of the particles in which the particles are charged at the inlet, and then the aerosol flows through an electric field. The particles follow different trajectories depending on their aerodynamic size and electrical charge [13]. In the aerodynamic particle sizer (APS), that is one of the main instruments employed in this work, the particles are accelerated. The velocity at the end of the acceleration process is measured with the transit time between optic detectors. Since the transit time depends on the particle Stokes number the aerodynamic size can be calculated. The particles are counted optically and then grouped in size bins [14]. These measurement methods produce data that give different physical information about the particles and then have to be carefully analyzed. Therefore several measurement techniques are usually required.

Lognormal distributions are representative of the particle natural distributions obtained from physical measurements [15] and their geometric mean and geometric standard deviation are characteristic parameters of those distributions. In the case of aerosols the number size distribution usually follows the lognormal distribution better than other distributions (such as normal distribution) because the particle diameters are never less than zero and the distribution on the bigger sizes have a longer tail [16]. In this work we measure mixtures of aerosols composed by several monodisperse aerosols and we characterize them by adjusting a sum of lognormal distributions and extracting the characteristics of those lognormal distributions (geometric mean and geometric standard deviation).

2 Measurements

2.1 Experimental setup

The experimental facility to generate and characterize the aerosol, named Experimental Plant for Aerosol Generation and Characterization (PECA), produces particles whose size is related to the expected size in case of accidents [17-19]. Inside the PECA vessel an ultrasonic chamber has been installed, the Mitigative System - Acoustic Agglomerator (MSAA). The aerosol is pushed through the intense ultrasound field generated in the MSAA and collected at the outlet of the PECA. During the process the measurements of the aerosol particle distribution at the inlet and at the outlet of the MSAA are carried out and the experimental conditions are monitored. The system has been described in detail elsewhere [20].

In the experimental work here reported the aerosols generated with concentrations up to 200 mg/m^3, the particle distribution was measured with an Aerodynamic Particle Sizer (APS) of TSI, and the MSAA generates a 21 kHz standing wave field inside the chamber with an average sound pressure level of 155 dB.

2.2 Experimental conditions

The aerosols used consisted of mixtures of primary SiO_2 particles of different sizes in all cases except in one experiment in which SiO_2 were mixed with TiO_2 particles. The SiO_2 are spherical mono disperse (GSD below 1.1) particles 0.3 µm, 1 µm and 2.5 µm in diameter and the TiO_2 particles were irregular polydisperse particles agglomerated with primary particles sized between 0.01 µm and 0.05 µm. Ten experiments were carried out under different experimental conditions summarized in Table 1. In the AAA1 and AAA2 experiments the aerosol was composed by monodisperse aerosols of 1 µm at different flows. Since the aerosol generator released the particles at the same mass/time rate, the increase in the flow implies a decrease in the aerosol mass concentration. Also higher flow implies less residence time in the ultrasonic field. The influence of the residence time and concentration has been also studied for poly-disperse aerosols with particles of 1 µm and 0.3 µm (experiments AAA4, AAA5, and AAA6). The experiments AAA1, AAA3, AAA4 and AAA7 aim to understand the influence of the mass proportion of SiO_2 particles of two sizes (0.3 and 1 microns) on aerosols with the same total mass concentration and the same residence time. The experiments AAA8 and AAA9 study the influence of bigger particles (2.5 µm) in the agglomeration process. Lastly the AAA10 experiment study the influence of very poly-disperse TiO_2 aerosol.

After achieving a good stabilization of the aerosol generation, by measuring particle distribution at the inlet by means of an ELPI device (electric-collector system) [14], the experiment is started. For each experimental condition of Table 1 four phases were considered. In the first phase (F1) no ultra sound field was applied to the aerosol. The second phase (F2) was equal to the first one but the ultrasound field was applied. Then the two phases were repeated (F1' and F2') to account for variations on experimental conditions like mass concentration and repetitivity. In the phase F2' of some experiments the ultrasound field was switched on and off to see clearly the influence of the ultrasonic energy. The APS measured the aerosol at the outlet for five minutes. The details of the experimental procedure are explained in more detail elsewhere [20].

Table 1 – Experimental variables of the experimental matrix

Name	Flow (kg/h)	Residence time (s)	Input Total Mass Concentration (mg/m^3)	Mass proportion of SiO_2 0.3 µm (%)	Mass proportion of SiO_2 1 µm (%)	Mass proportion of SiO_2 2.5 µm (%)	Mass proportion of TiO_2 (%)
AAA2	100	10	25	0	100	0	0
AAA6	100	10	25	75	25	0	0
AAA5	50	20	50	75	25	0	0
AAA4	12.5	80	200	75	25	0	0
AAA1	12.5	80	200	0	100	0	0
AAA3	12.5	80	200	50	50	0	0
AAA7	12.5	80	200	90	10	0	0
AAA8	12.5	80	200	0	75	25	0
AAA9	12.5	80	200	50	30	20	0
AAA10	12.5	80	200	50	30	0	20

2.3   APS Mesurements

At the outlet of the ultrasonic chamber the Aerodynamic Particle Sizer (APS) measured the particle size distributions in the range 0.5 to 20 μm in intervals of dlogDp of 0.03 every second. The typical uncertainty of the number distribution of a single channel of the APS is 18% [13]. The aerodynamic diameter uncertainty ranges between 18% and 20% [13]. In our measurements the relative standard deviation of particle number concentration for each experimental phase ranged from 2% to 34% with an average of 10% and the relative standard deviation of the ACMD ranged from 0% to 25% with a mean of 3%. The APS number distribution measured by the APS was converted to concentration/dlogDp from the count number. Following the APS specifications this calculation was done by using the equations 1, 2 and 3, where n is the channel particle concentration, c is the particle count given by the APS, t the sample time, Q Sample Flow Rate, φ sample dilution factor, η is the channel sample Efficiency Factor (taken as constant for all channels), Np total particle concentration given by the APS software and the summation goes to all the channels.

$$n = \frac{c}{t\,Q}\frac{\phi}{\eta} \tag{1}$$

$$N_p = \sum n \tag{2}$$

$$\frac{\phi}{t\,Q\,\eta} = cte = \frac{N_p}{\sum_1^u c} \tag{3}$$

Then the concentration was adjusted by the dilution factor (100 for all the experiments).

In the distributions (Figure 1) two particle sizes could be seen clearly, one around 0.53 μm and another one around 1.5 μm. In the cases in which there were also 2.5 μm SiO_2 particles a peak around 2.5 μm was also observed.
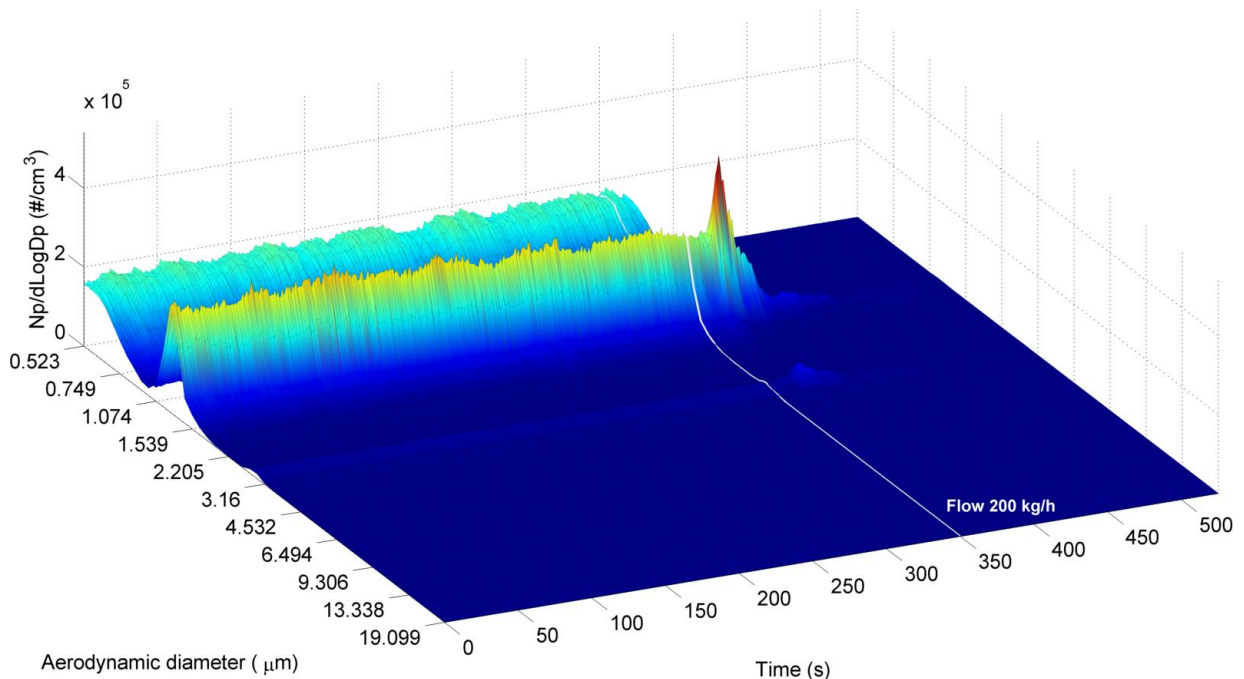

Figure 1 – AAA9 particles 2.5 APS measurement during the F1' phase

4

As an example of the ultrasound effect Figure 2 shows the APS measurements of the F2' phase of the AAA9 test in which the ultrasound field was switched on and off. During the time in which the ultrasound is switched off the peaks rise and when the ultrasound is switched on again the particles agglomerate and the peaks of the distribution drop.
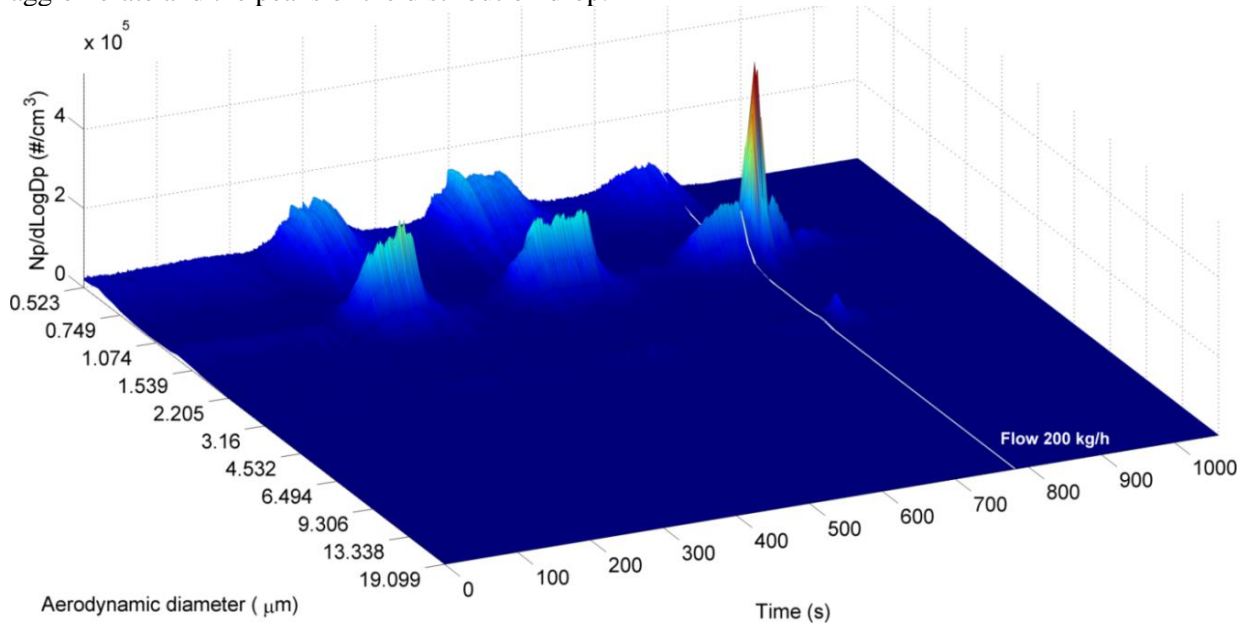
Figure 2 – AAA9 APS measurement during the F2' phase

In the AAA10 test the very small primary particles of TiO_2 were not clearly seen in the distribution mainly because they were outside the range of the APS instrument (Figure 3) but in general the peaks of the graphics correspond to the sizes of the particles introduced by the particle generation system at the inlet.
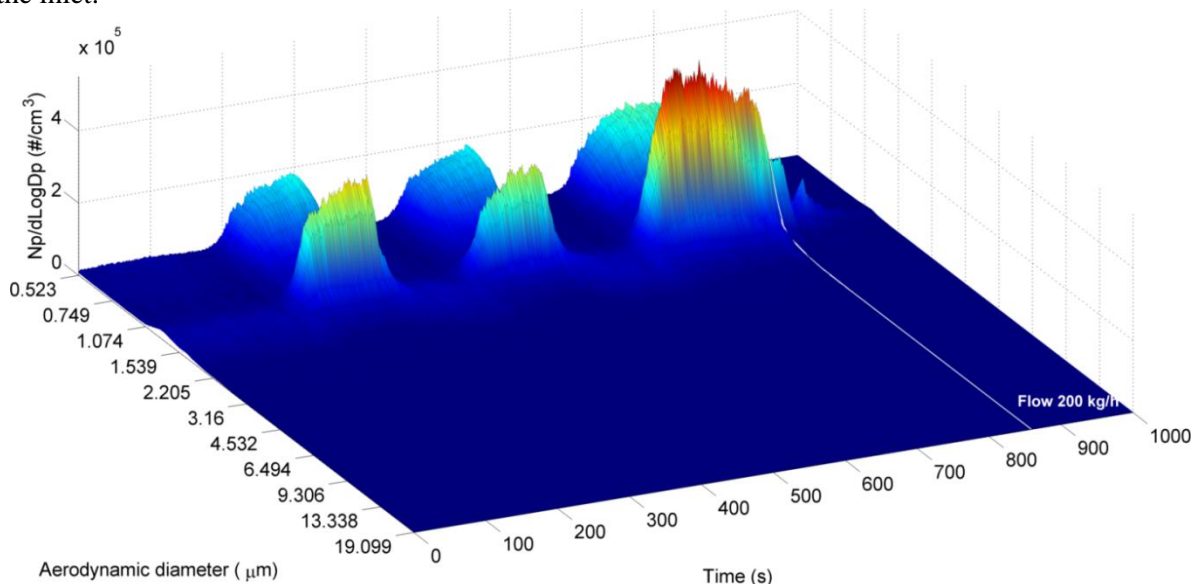
Figure 3 – AAA10 APS measurement during the F2' phase

3   Distribution characterization

3.1   Distribution characterization (AMMD)

The mass distribution was calcualted for each bin (M_{bin}) from the APS aerodynamic diameter count distribution with the equation 4 where D_p is the median diameter of the particles of the bin, ρ is the density of the particles, and Np_{bin} the count number of that bin.

$$M_{bin} = Np_{bin} \frac{\pi}{6} D_p^3 \rho \tag{4}$$

The distribution was characterized by the median mass distribution factor (AMMD) that was calculated by its definition as the number that separates half the upper samples to the lower ones. Since the data was binned the calculation was done by the following steps. First the cumulative frequency distribution was constructed. Then the bin that contains the median was found as the first bin whose cumulative frequency equals at least *n/2*. Then the equation 5 was used to compute the median where *L* is the lower boundary of the determined median bin, *i* is the width of the median bin, n the total frequency, *F* the cumulative frequency before the class median and *f_m* the frequency of the median bin.

$$Median = L + i \frac{n/2 - F}{f_m} \tag{5}$$

The geometric standard deviation (GSD) was then calculated by its definition (Eq. 6). Where the summation goes for all bins, *n* is the population of that bin, *x* is the given bin diameter, $\bar{x}_g$ the geometric mean of the distribution and *N* the total number. Then the relative increase of a magnitude X was calculated and averaged for two successive phases (F1-F2 and F1'-F2').

$$GSD = exp\left(\sqrt{\left[\frac{\sum n(Ln\,x - ln\,\bar{x}_g)^2}{N}\right]}\right) \tag{6}$$

Table 2 shows the results for the changes of the AMMD and GSD. The results show that there was a general displacement of the AMMD toward higher values, but in some cases the AMMD change did not reflect the acoustic agglomeration (AAA6 and AAA7). This could be because the APS didn't measured completely the 0.3 μm particles and the distribution changes were not well measured with the AMMD. For this purpose two other descriptive analysis, shown in the following sections, were made.

Table 2 – Changes on the AMMD and GSD for each experiment

Experiment Name	Experimental variables					Results	
	Flow (kg/h)	% Mass of SiO$_2$ 0.3 μm particles	% Mass of SiO$_2$ 1 μm particles	% Mass of SiO$_2$ 2.5 μm particles	% Mass of TiO$_2$ particles	Δ AMMD	Δ GSD
AAA1	12.5	0	100	0	0	-6.2%	10.8%
AAA2	100	0	100	0	0	-1.1%	-1.1%
AAA3	12.5	50	50	0	0	21.5%	16.5%
AAA4	12.5	75	25	0	0	26.1%	9.9%
AAA5	50	75	25	0	0	-2.5%	4.4%
AAA6	100	75	25	0	0	-1.1%	2.3%
AAA7	12.5	90	10	0	0	-0.7%	-11.4%
AAA8	12.5	0	75	25	0	-3.7%	-4.4%
AAA9	12.5	50	30	20	0	21.9%	4.6%
AAA10	12.5	50	30	0	20	36.3%	26.8%

3.2   Distribution characterization, (Curve Fitting)

To compare the distributions the mean distribution values of each APS phase was calculated during the first three minutes. Those values were used to characterize the aerosol particle size distributions. Figure 4 shows the four mean distributions for the test AAA4 with areas that represent the standard deviation of the mean values.
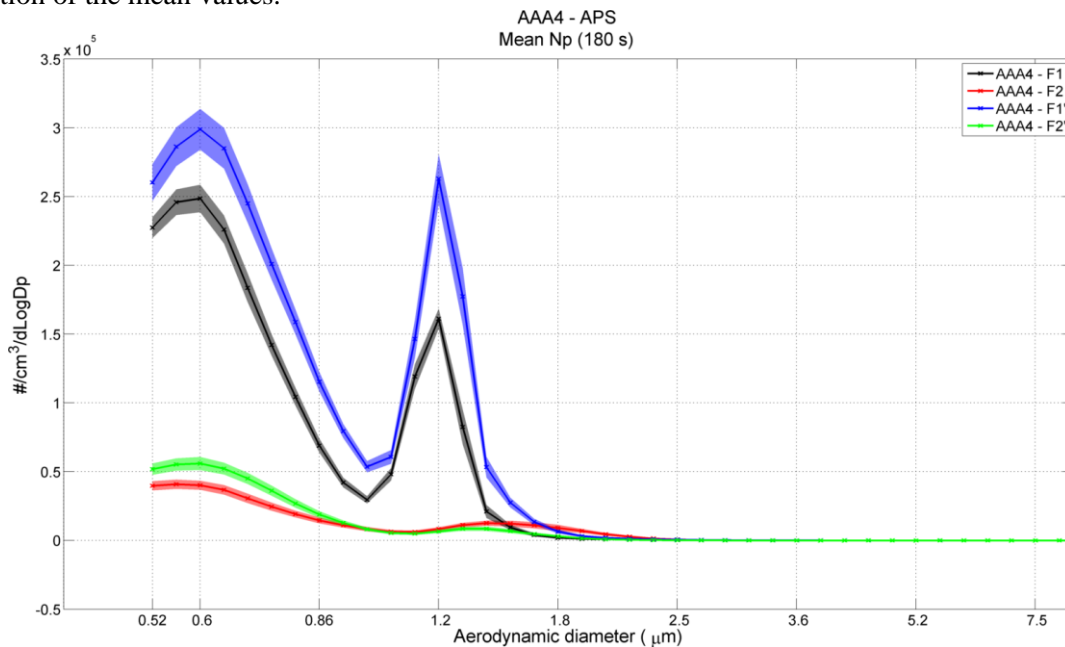

Figure 4 – Number distribution of test AAA4

To study with more precision the higher diameter particles the distributions were changed to aerodynamic mass particle distributions. Fig. 5 shows the mass distribution graph for the four APS phases of the AAA4 test including the standard deviation.
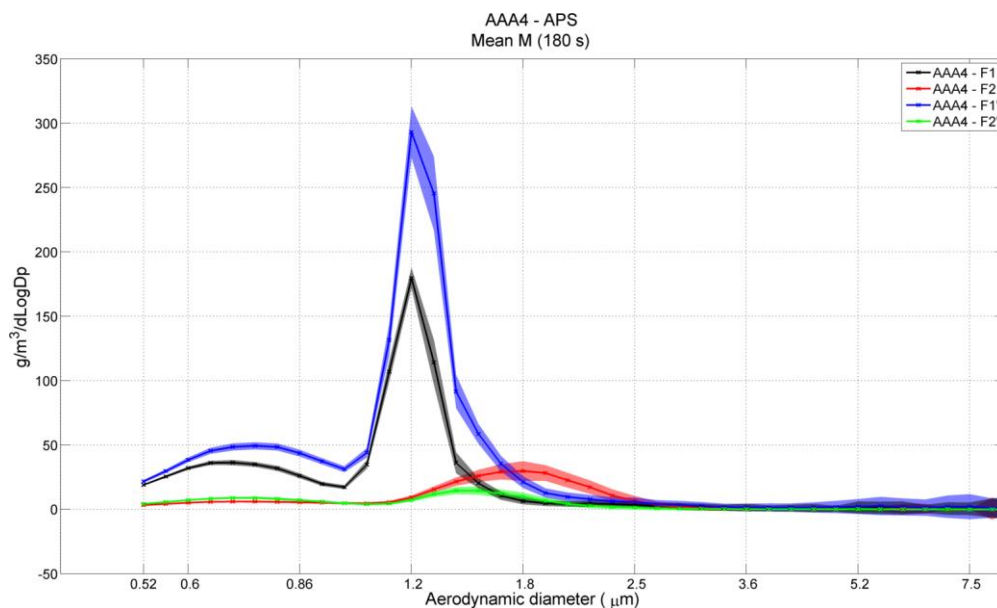

Figure 5 – Mass distribution of test AAA4

To study the ultrasonic effect on the different particles sizes sums of lognormal distributions were adjusted by least squares to the measured distributions by equation 9.

$$f = \sum A\, lognormal\,(\mu, \sigma) = \sum \frac{1}{x\sigma\sqrt{pi\,2}} e^{-\frac{(\ln x - \mu)^2}{2\sigma^2}} \tag{9}$$

A number of lognormals equal to the number of types of particles (0.3 μm, 1 μm 2.5 μm and TiO2) introduced in the system were selected. If the adjustment was not able to produce a lognormal centered in each particle diameter the the number of lognormal terms was increased till a lognormal centered in each particle diameter was found. To characterize each particle diameter type the lognormal that was centered in the particle diameter of the first distribution sum was used. Then the GSD and median of those lognormals were calculated. Figure 6 shows the result of the adjustement for experiment AAA4.

The shifts of the mass distribution adjusted peaks are summarized in Table 4 where the R Pearson and the relative sum of squared errors (RSSE) are also presented in the right columns. The distribution corresponding to the 0.3 μm particles does not experiment big changes in median, probably because the small particles were no measured completely by the APS and also because there was very little agglomeration with themselves. As predicted by the orthokinetic effect the agglomeration was produced mainly between 0.3 particles and 1 μm particles, as it is shown by the shift on the distributions for the 1 μm. In the cases in which the flow rate was low and the particle concentration was high the ultrasonic agglomeration was more clearly observable. In those cases the increase in AMMD was up to 37% and the corresponding increase in the GSD was up to 17%. These increases reflect a broadening of the particle size distribution as shown in Figure 6 for the test AAA4.
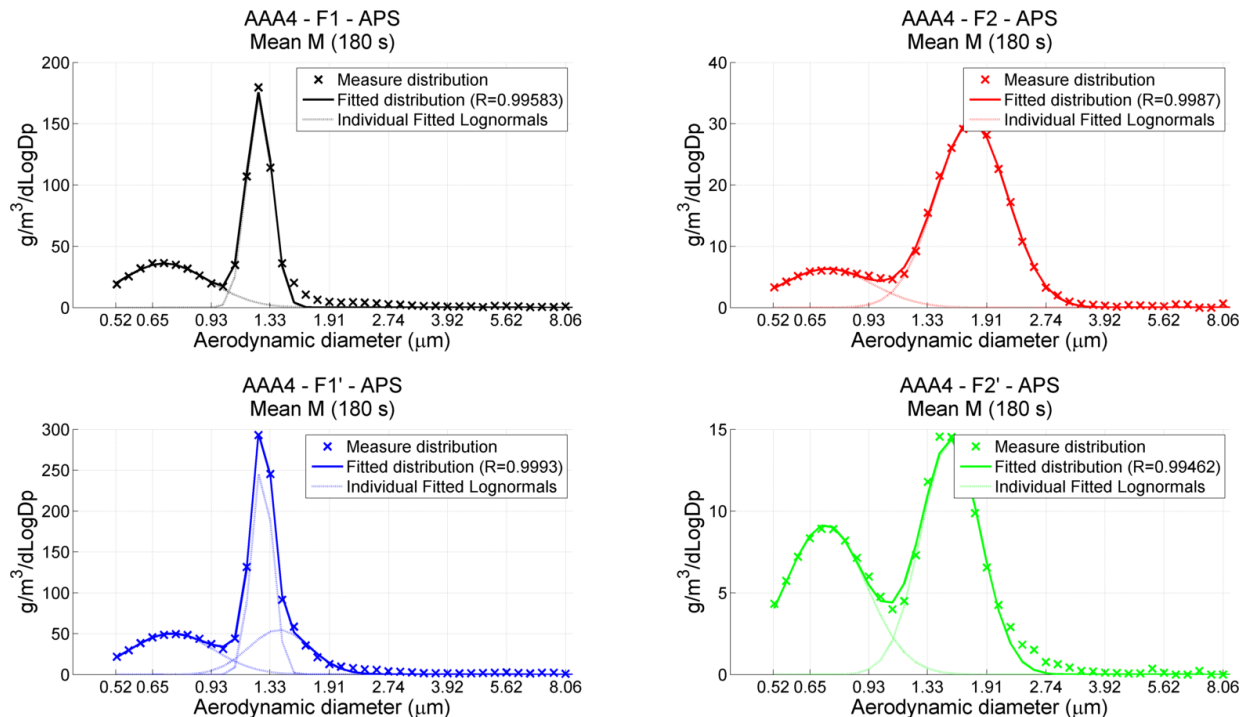

Figure 6 – Adjusted distributions for AAA4 tests

Table 4 – Relative increases of AMMD and GSD of the adjusted distributions

Experiment	Size and GSD Changes						Adjustment Error	
	Δ Median (%)	Δ GSD (%)	Δ Median (%)	Δ GSD (%)	Δ Median (%)	Δ GSD (%)	R	RSSE
	SiO$_2$ 0.3 µm		SiO$_2$ 1.0 µm		SiO$_2$ 2.5 µm			
AAA1			-12.2	-9.5			0.9980	0.0004
AAA2			-1.8	-0.3			0.9910	0.0013
AAA3	1.5	5.8	28.0	16.4			0.9991	0.0002
AAA4	0.5	-0.3	34.6	12.7			0.9971	0.0004
AAA5	8.4	6.4	3.4	4.2			0.9990	0.0002
AAA6	-4.2	-3.0	-1.0	0.6			0.9994	0.0002
AAA7	18.6	3.7	27.9	14.2			0.9967	0.0004
AAA8			-4.2	-4.2	-0.4	-67.7	0.9993	0.0003
AAA9	4.8	2.0	23.3	15.3	4.6	-87.3	0.9942	0.0005
AAA10	-100.0	-100.0	37.0	15.3			0.9970	0.0005

4   Conclusions

To characterize the acoustic aerosol agglomeration by measuring the aerodinamic size number distributions is a complex task that requires to extract several parameters. The AMMD is a good factor to characterize the aerosol particle diameter but fails to characterize the finner details. Fitted lognormal distributions can approximate the distributions with a very low residual. The parameters obtained with this method give more information and insight of the distributions and about the AAA process. The particle distribution changes show that the smaller particles agglomerate with the big ones producing an increase of the AMMD for only the bigger particles.

Acknowledgements

References

[1] J.A. Gallego-Juárez and K. F. Graff, Power Ultrasonics, Applications of High-Intensity Ultrasound, ISBN: 978-1-78242-028-6

[2] D. Zhou, Z. Luo, M. Fang, H. Xu, J. Jiang, Y. Ning, Z. Shi, *Preliminary Experimental Study of Acoustic Agglomeration of Coal-fired Fine Particles*, Procedia Engineering, Volume 102, 2015, Pages 1261-1270

[3] H.S. Patterson and W. Cawood, Phenomena in sounding tube. 1931 Nature 127 (3209) 667

[4] J.A. Gallego-Juarez, G. Rodriguez-Corral, L. Gaete-Garreton, An ultrasonic transducer for high power applications in gases, Ultrasonics, Volume 16, Issue 6, 1978, Pages 267-271, ISSN 0041-624X

[5] J. A. Gallego-Juárez, E. Riera-Franco De Sarabia, G. Rodríguez-Corral, T. L. Hoffmann, J. C. Gálvez-Moraleda, J. J. Rodríguez-Maroto, F. J. Gómez-Moreno, A. Bahillo-Ruiz, M. Martín-

Espigares, M. Acha, Application of Acoustic Agglomeration to Reduce Fine Particle Emissions from Coal Combustion Plants Environmental Science & Technology 1999 33 (21), 3843-3849

[6] D. T. Shaw, N. Rajendran, Application of Acoustic Agglomerators for Emergency Use in Liquid-Metal Fast Breeder Reactor Plants, Nuclear Science and Engineering / Volume 70 / Number 2 / May 1979 / Pages 127-134

[7] H.-J. Allelein, A. Auvinen, J. Ball, S. Güntay, L. Enrique Herranz, A. Hidaka, A. V. Jones, M. Kissane, D. Powers, G. Weber, *State-Of-The-Art Report On Nuclear Aerosols*, Nuclear Energy Agency Committee On The Safety Of Nuclear Installations, NEA/CSNI/R(2009)5

[8] E.P. Mednikov, Acoustic coagulation and precipitation of aerosols, New York, Consultants Bureau, 1965

[9] N.L. Shirokova, Aerosol coagulation, in Rozenberg LD, Volume 2, Physical Principles of Ultrasonic Technology, New York, Plenum Press, 1973, 475-539

[10] S. Temkin, Gas dynamic agglomeration of aerosols. I. Acoustic waves, Phys Fluids, 6, 1994 2294-2303

[11] D.T. Shaw, Acoustic agglomeration of aerosols, Recent developments in aerosol science, New York, John Wiley and Sons, 1978, 279-319

[12] A. Järvinen, M. Aitomaa, A. Rostedt, J. Keskinen, J. Yli-Ojanperä, 2014. Calibration of the new electrical low pressure impactor (ELPI+). J. Aerosol Sci. 69, 150–159

[13] G. Buonanno , M. Dell'Isola , L. Stabile , A. Viola, Uncertainty Budget of the SMPS–APS System in the Measurement of PM1, PM2.5, and PM10, Aerosol Science and Technology Vol. 43, Iss. 11, 2009

[14] J. Pagels, , A. Gudmundsson, E. Gustavsson, L. Asking, M. Bohgard, 2005. Evaluation of Aerodynamic Particle Sizer and Electrical Low-Pressure Impactor for Unimodal and Bimodal Mass-Weighted Size Distributions. Aerosol Sci. Technol. 39, 871–887

[15] O'Neill N. T., A. Ignatov, B. N. Holben, T. F. Eck, The lognormal distribution as a reference for reporting aerosol optical depth statistics; Empirical tests using multi-year, multi-site AERONET Sunphotometer data, Geophysical Research Letters, October, 2000.

[16] William C. Hinds, Aerosol Technology: Properties, Behavior, and Measurement of Airborne Particles, ISBN: 978-0-471-19410-1

[17] E. I. Kauppinen, R. E. Hillamo, S. H. Aaltonen and K. S. Sinkko, Radioactivity Size Distributions of Ambient Aerosols in Helsinki, Finland, during May 1986 after the Chernobyl Accident: Preliminary Report, Environ.cl. Technol. 1986, 20, 1257-1259

[18] H. Malá, P. Rulík, V. Bečková, J. Mihalík, M. Slezáková, Particle size distribution of radioactive aerosols after the Fukushima and the Chernobyl accidents, Journal of Environmental Radioactivity, Volume 126, December 2013, Pages 92-98

[19] N. Yamaguchi, M. Mitome, A.H. Kotone, M. Asano, K. Adachi, and T. Kogure, Internal structure of cesium-bearing radioactive microparticles released from Fukushima nuclear power plant, Scientific Reports 6, Article number: 20548 (2016) doi:10.1038/srep20548M.

[20] Aleixandre, E. Riera, R. Delgado-Tardáguilla, L.E. Herranz, V.M. Acosta, A. Pinto, I. Martínez, J.A. Gallego-Juárez, Characterization Of The Changes Of The Particle Size Distribution Of Different Aerosols During An Acoustic Agglomeration Process, Conferencias y Comunicaciones del 46º Congreso Español de Acústica, Encuentro Ibérico de Acústica y Simposio Europeo de Acústica Virtual y Ambisonics. ISBN: 978-84-87985-26-3. ISSN: 2340-7441 (Versión Digital). Valencia. España. Octubre, 2015